Millimetre-wave Electro-Optic Modulator with Quasi-Phase-Matching Array of Orthogonal-Gap-Embedded Patch-antennas on Low-k Dielectric Material

Yusuf Nur Wijayanto[1], Atsushi Kanno[1], Hiroshi Murata[2], Sinya Nakajima[1], Tetsuya Kawanishi[1] and Yasuyuki Okamura[2]

[1]*National Institute of Information and Communications Technology, 4-2-1 Nukui-Kitamachi, Koganei, Tokyo, 184-8795, Japan*

[2]*Osaka University, 1-3 Machikaneyama, Toyonaka, Osaka, Japan*

Keywords: Electro-optic Modulator, Patch-antenna Array, Quasi-phase-Matching, Low-*k* Dielectric, Millimetre-wave.

Abstract: In Fibre-Wireless (Fi-Wi) links, conversion devices between wireless microwave/ millimetre-wave and lightwave signals are required. In this paper, we propose a wireless millimetre-wave-lightwave signal converter using an electro-optic (EO) modulator with Quasi-Phase-Matching (QPM) array of orthogonal-gap-embedded patch-antennas on a low-*k* dielectric material. Wireless millimetre-wave signals can be received and converted directly to lightwave signals using the proposed device. It can be operated with no external power supply and extremely-low millimetre-wave losses. The orthogonal-gap-embedded patch-antennas can be used for receiving dual-linearized or circular polarizations of wireless millimetre-wave signals. The QPM array structure can be adopted for enhancing modulation efficiency by transit-time effects consideration. Structure, analysis, and experimental of the proposed device are discussed for 40GHz operational millimetre-wave bands.

1 INTRODUCTION

Recently, wireless communication has been implemented and used for transferring data to mobile devices. Microwave bands are used widely for carrying data through air medium with several wireless communication standards such as Wi-Fi, WiMAX, LTE, and so on (Abichar, 2006) (Akyildiz, 2010). Since demand of high quality data transfers using mobile devices is always increase time by time, the microwave bands will be saturated in the near future. Scientists and researchers are looking for solving the future problem by minimizing the data, saving used frequency spectra, enlarging operational bandwidth, and so on (Mendeiros, 2014) (Lu, 2014) (Pi, 2011).

In order to enlarge the operational bandwidth, high operational microwave frequency into millimetre-wave or sub-millimetre-wave bands are promising to use for carrying large data with high transfer speed. The millimetre-wave bands have relatively large propagation loss in air and metal cables (Rec. ITU-R P.676-5, 2001) (Iezekiel, 2009). Therefore, short distance wireless millimetre-wave communication in pico/ femto-cells can be developed. Since coverage area of pico/ femto-cells is small, networking of pico/ femto-cells can be adopted for enlargement of the coverage area. The pico/ femto-cell networks can be connected using low propagation loss optical fibres as backhaul networks by adopting microwave-photonic technology (Shi, 2011).

Microwave-photonic technology is a combination technology where microwave and lightwave bands are operated simultaneously by considering their advantages such as high mobility, large bandwidth, no induction, and so on (Seed, 2002). The technology can be implemented on Fiber-Wireless (Fi-Wi) links since wireless microwave and optical fibre communication are used together. In order to realize the Fi-Wi link, converters between microwave and lightwave signals are highly required. A high-speed photo-detector can be used for converting lightwave signals to microwave signals (Watanabe, 2000). As the other one, microwave signals can be converted to lightwave signals by use of a high-speed optical modulator (Shinada, 2007).

Wijayanto Y., Kanno A., Murata H., Nakajima S., Kawanishi T. and Okamura Y..
Millimetre-wave Electro-Optic Modulator with Quasi-Phase-Matching Array of Orthogonal-Gap-Embedded Patch-antennas on Low-k Dielectric Material.
DOI: 10.5220/0005325200050013
In *Proceedings of the 3rd International Conference on Photonics, Optics and Laser Technology* (PHOTOPTICS-2015), pages 5-13
ISBN: 978-989-758-093-2

Generally for wireless applications, a converter from wireless microwave/ millimetre-wave to lightwave signals is composed of wireless microwave/ millimetre-wave antennas and optical modulators (Sheehy, 1993). The antennas are used for receiving wireless microwave/ millimetre-wave signals. Then, the received microwave/ millimetre-wave signals are transferred to the optical modulators by a connection line, such as a coaxial cable. Therefore, the microwave/ millimetre-wave signals are modulated in lightwave signals propagated on optical fibres. However, microwave/ millimetre-wave signal distortion and decay might occur in the connection line when an operational frequency becomes high.

Integration of microwave/ millimetre-wave antennas and optical modulators fabricated on an electro-optic (EO) crystal are also developed for reducing microwave/ millimetre-wave signal distortion and decay (Bridge, 1991) (Murata, 2012). They are composed of planar antennas, connection lines, and resonant electrodes with simple and compact device structures. Since several microwave/ millimetre-wave planar electrodes on the substrate, completely impedance matching is required to obtain effective microwave/ millimetre-wave resonance. The tuning of them are rather difficult and low microwave/ millimetre-wave losses might be still induce along the connection line and their coupling.

New fusion of microwave/ millimetre-wave antennas and EO modulators were proposed (Wijayanto, 2011) (Wijayanto, 2012). Patch-antennas embedded with a narrow-gap were fabricated on EO crystal as the substrate. Displacement current and microwave/ millimetre-wave electric field across the gap can be used for EO modulation. Precise tuning is not required since only patch-antennas on the substrate. Therefore, extremely low microwave/ millimetre-wave signal distortion can be achieved using the fusion structures with a simple and compact structure. EO modulators using the fusion structures in an array structure were also reported for enhancing modulation efficiency by considering transit-time effect (Yariv, 1989). In high operational frequency, the patch-antennas becomes small. Therefore, antenna gain becomes small and microwave/ millimetre-wave-lightwave electric field interaction length becomes short. The reported devices are operated effectively for a linear microwave/ millimetre-wave polarization.

In this paper, a millimetre-wave EO modulator with a quasi-phase-matching (QPM) array of orthogonal-gap-embedded patch-antennas on a low-*k* dielectric material is proposed. By using low-*k* dielectric material as an antenna substrate, a large patch-antenna size can be realized for increasing antenna gain and enhancing millimetre-wave electric field strength across the gaps and enlarging interaction length between millimetre-wave and lightwave electric fields. Therefore, modulation efficiency enhancement can be obtained. Further enhancement of the modulation efficiency can be achieved using the QPM array structure by considering transit-time effect. Additionally, the proposed device can be operated for dual linear or circular millimetre-wave polarizations.

The device structure, operational principle, analysis, fabrication, and measurement of the proposed millimetre-wave EO modulator are presented for operation with 40GHz millimetre-wave bands.

2 EO MODULATOR

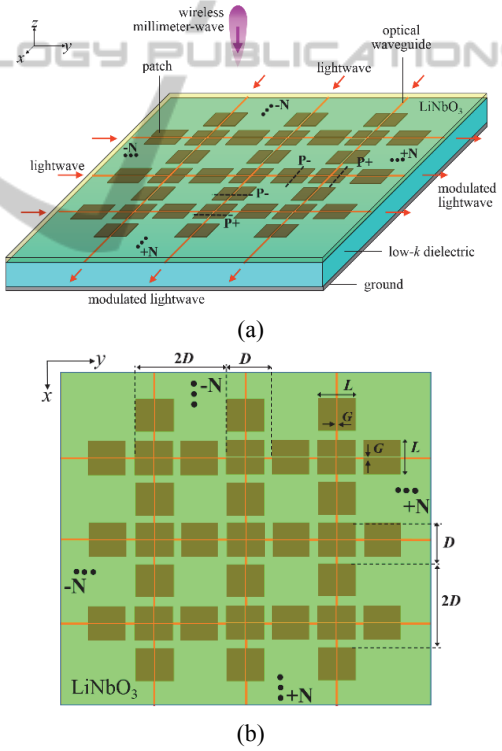

Figure 1: Structure of QPM array of patch-antennas with orthogonal-gaps on low-*k* dielectric material stacked with EO modulator, (a) whole and (b) top views.

Figure 1 shows a structure of the proposed device. It consists of a QPM array of patch-antennas with orthogonal-gaps fabricated on a low-*k* dielectric material stacked with a thin $LiNbO_3$ optical modulator. The patch electrodes are inserted between

the $LiNbO_3$ optical crystal and low-k dielectric material. The patch electrode length, L, is set at a half wavelength of the designed millimetre-wave. The gap width, G, is set in micrometre order (<10μm). The patch electrodes are set in an array structure by considering a QPM method with a distance of D. Since a z-cut $LiNbO_3$ optical crystal is used, optical waveguides are located on a one side of the gap edge as shown in cross-sectional view of Figure 2. The gap position refer to the optical waveguide are slightly shifted for satisfying the QPM method. A buffer layer is also inserted between the $LiNbO_3$ optical crystal and patch electrodes. The reverse side of the low-k dielectric material is covered with a ground electrode.

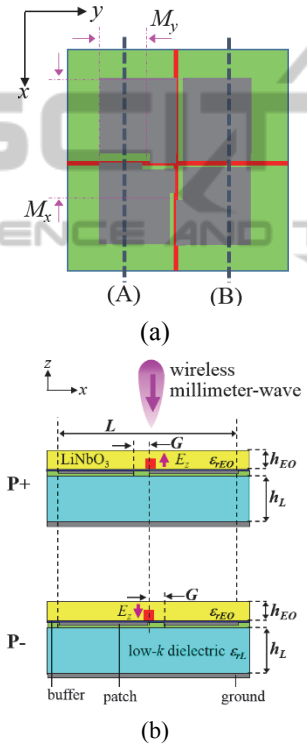

Figure 2: Structure of meandering gaps for polarization inversed structure, (a) top and (b) cross-sectional views.

When a wireless millimetre-wave signal is irradiated to the device, standing-wave currents are induced on the patch electrode surface (Lefort, 1997) (Gupta, 2004). By embedding orthogonal-gaps at the centre of the patch electrodes, millimetre-wave displacement current and strong electric field are induced across the orthogonal-gaps due to current flow continuity (Rodriguez-Berral, 2011). The induced millimetre-wave electric field can be used for optical modulation thru the Pockels EO effect of $LiNbO_3$ optical crystal. When lightwave propagating in the orthogonal optical waveguides located on the orthogonal-gaps are modulated by the radiated wireless millimetre-wave signal. Since the gap width is relatively much smaller than the patch electrode size, the patch-antenna characteristics are not changed. Generally, modulation efficiency improvement can be obtained using an array structure. However, the spacing between patch electrodes is required relatively large owing to the transit-time effect (Yariv, 1989). QPM methods can be adopted to reduce the spacing of about half. Therefore, twice modulation efficiency can be obtained using QPM array structure in the same device length, since the patch electrodes number becomes double.

3 ANALYSIS

3.1 Millimetre-wave Analysis

3.1.1 Displacement Current

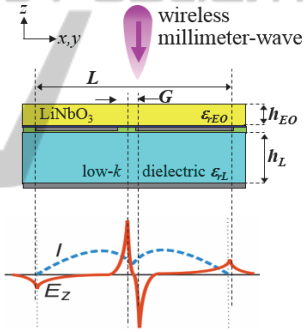

Figure 3: Millimetre-wave current and electric field profiles of the proposed device.

When a wireless millimetre-wave signal is irradiated to the standard patch-antennas with no gap, a standing-wave millimetre-wave surface current is induced on the patch electrodes. Then, orthogonal narrow gaps are introduced at the centre of the patch electrode as shown in Figure 3. Owing to the requirement of current continuity on the patch electrode, millimetre-wave displacement current and strong electric field are induced across the gap. The induced millimetre-wave electric field across the gap is obtained by time integration of the displacement current. Therefore, it can be expressed as

$$E_m(t) = E_0 \cos(\omega_m t) \quad (1)$$

The millimetre-wave current and electric field profiles of the proposed device are illustrated in Figure 3.

3.1.2 Patch-antenna Size

In order to consider for obtaining large antenna gain, it can be achieved by enlarging patch electrode fabricated on a low-*k* dielectric material as the antenna substrate. In general, a patch electrode size is inversely proportional to the designed operational frequency of wireless millimetre-wave signals. It is also inversely proportional to square root of substrate effective dielectric constant (Gupta, 2004).

The patch electrode size can be enlarged by reducing the effective dielectric constant. In order to reduce the effective dielectric constant of the substrate, it can be realized using a thin high-*k* EO crystal bonded with a low-*k* dielectric material as shown in Figure 1. By using a bonded material structure with a thin EO crystal, the effective dielectric constant becomes low.

3.1.3 EO Crystal Types

The EO crystal orientation, the distribution of the millimetre-wave electric field across the orthogonal-gaps, and position of the optical waveguide must be taken into account for achieving effective operation. The orthogonal optical waveguides should be set on one side of the gap edge as shown in Figure 2, since a *z*-cut $LiNbO_3$ optical crystal is used in the analysis.

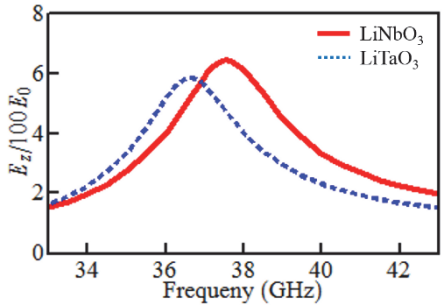

Figure 4: The calculated millimetre-wave electric field across the gap for *z*-cut $LiNbO_3$ (solid-line) and $LiTaO_3$ (dashed line).

The induced millimetre-wave electric field across the gaps was calculated using electromagnetic software analysis. The optical crystal thickness was set 80μm and low-*k* dielectric material thickness was set 130μm with dielectric constant of 3.5. The length and width of the patch electrodes with gold metal were set 1.6mm. A gap with 10μm-wide was located at the centre of the patch electrodes. Ultraviolet adhesive glue as a buffer layer was also inserted between the bonded structures. The calculated electric fields across the gap are shown in Figure 4 for *z*-cut $LiNbO_3$ (solid-line) and $LiTaO_3$ (dashed line). The millimetre-wave operational frequencies are shifted due to different effective dielectric constant of the devices with bonded structure between anisotropic $LiNbO_3$/ $LiTaO_3$ crystal and low-*k* material. Based on the result, we expected that the proposed device using *z*-cut $LiNbO_3$ crystal can be used for enhancing modulation efficiency.

3.1.4 EO Crystal Thickness

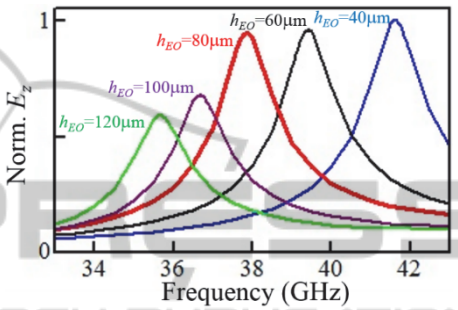

Figure 5: The calculated millimetre-wave electric field across the gap for *z*-cut $LiNbO_3$ crystal dependences.

Figure 5 shows the calculated millimetre-wave electric field magnitude across the gap as a function of operational frequency for several *z*-cut $LiNbO_3$ optical crystal thicknesses. The peak frequency is shifted due to different effective dielectric constant of the proposed device by changing the $LiNbO_3$ optical crystal thickness. When the *z*-cut $LiNbO_3$ crystal thickness becomes thin, operational frequency becomes high and millimetre-wave electric field strength becomes large. It is promising also for obtaining large modulation efficiency.

3.1.5 Millimetre-wave Polarization

Figure 6 shows the calculated electric field distributions in the *z*-component for the top view. We can see that the strong millimetre-wave electric field is induced across the gaps. The strongest millimetre-wave electric field is induced when the millimetre-wave polarization is perpendicular to the gaps. Almost no millimetre-wave electric field is induced, when the millimetre-wave polarization is parallel to the gaps. When the millimetre-wave polarization is not completely perpendicular or parallel to one of the gap, the millimetre-wave electric field is induced across the two orthogonal-gaps. The magnitude of millimetre-wave electric field across the gap depends on the millimetre-wave polarization condition.

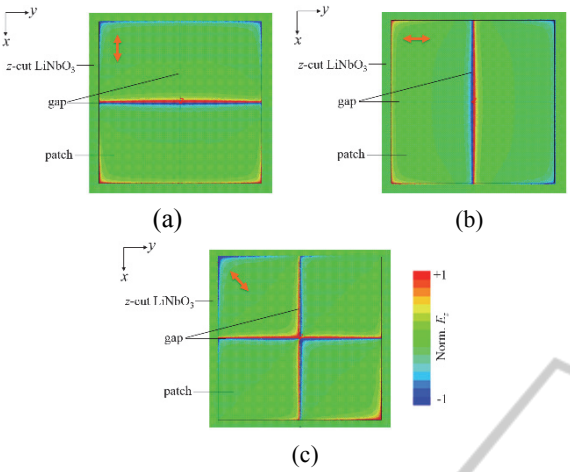

Figure 6: Calculated millimetre-wave electric field distribution in the *z*-component for (a) *x*-, (b) *y*-, and (c) *xy*-polarizations (diagonal).

3.2 Optical Modulation

3.2.1 Transit-time Effect

For an array of gap-embedded patch electrodes, the temporal phases of the millimetre-wave signal supplied to the gap-embedded patch electrodes are changed according their distance, D, and the wireless irradiation angle, θ_x and θ_y. When a lightwave propagates in the optical waveguide, the millimetre-wave electric field as would be observed by the lightwave can be expressed by following equation with taking into account the transit-time of the lightwave

$$E^h_{m-light}(y,\theta_y) = E_0 \cos(k_m n_g y) + 2Dh(k_m n_0 \sin\theta_y + \varphi) \quad (2)$$

where k_m is the wave number of the millimetre-wave, n_g is the group refractive index, h denotes the number of the gap-embedded patch electrodes, D is a distance of the patch electrodes ($D = \Lambda_m/2n_g$), n_0 is the refractive index of the millimetre-wave in air (=1), and φ is an initial phase of the lightwave ($\varphi = k_m n_g y'$). The millimetre-wave electric fields as would be observed by the lightwave are shown by the sinusoidal-curve in Figure 7.

The proposed QPM device is an optical phase modulator, therefore the modulation efficiency, $\Delta\phi$ from the wireless millimetre-wave signal to the optical signal is proportional to power ratio between lightwave carrier and sidebands, when $\Delta\phi << 1$. The modulation efficiency is calculated by the integration of millimetre-wave electric field as would be observed by the lightwave along the gap-embedded patch electrodes, it can be expressed as following equation for optical waveguide along *y*-axis,

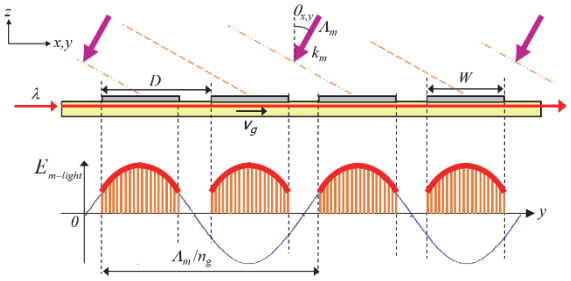

Figure 7: Operational principle of QPM EO modulators under irradiation of a wireless millimetre-wave signal angle of $\theta_{x,y}$ degrees. Modulation efficiency corresponds to the shaded-areas.

$$\Delta\phi(\theta_y) = \frac{\pi r_{33} n_e^3}{\lambda} \Gamma \sum_{h=-N}^{N} \int_0^W P(y)\, E^h_{m-light}(y,\theta_y)\, dy \quad (3)$$

where λ is the wavelength of lightwave propagating in the optical waveguides, r_{33} is the EO coefficient, n_e is the extraordinary refractive index of the substrate, Γ is a factor expressing the overlapping between the induced millimetre-wave and the lightwave electric field, W are the width of the patch electrodes as the interaction length of the millimetre-wave and lightwave electric field, and N is the number of gap-embedded patch electrodes in an array structure. $P(y)$ expresses the polarization of the millimetre-wave electric field in the *z*-component under the gap edge along the optical waveguide. The modulation index of the QPM structure corresponds to the sum of the shaded areas of the millimetre-wave electric field observed by lightwave in Figure 7. Since the modulation index is also a function of wireless irradiation angle, θ, the directivity in the modulation efficiency can be also calculated using Equation (3).

3.2.2 QPM Array

The millimetre-wave electric fields in the *z*-component between two-edges of gaps have different polarities (Rodriguez-Berral, 2011). The different polarities enable us to obtain the polarization-inversed structure for the QPM condition. The polarization-inversed structures on a *z*-cut EO crystals are obtainable by switching spatial relationship between the gap edge and optical waveguide along the gap-embedded patch electrodes.

In order to obtain polarization-inversed structure, meandering gaps can be adopted as shown in Figure

2. The gaps are meandered on straight optical waveguide by considering transit-time effect. Therefore, it can be used for recovering optical modulation degradation due to miss-matching between millimetre-wave and lightwave electric fields.

3.2.3 Wireless Irradiation Angle

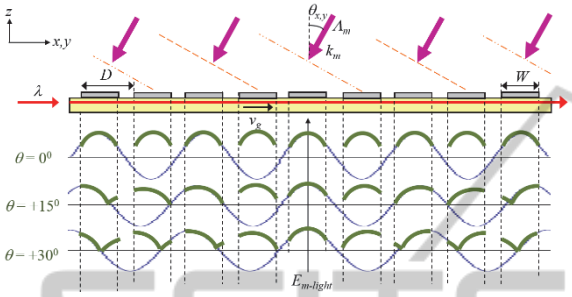

Figure 8: Typical patterns of patch electrodes with meandering gaps.

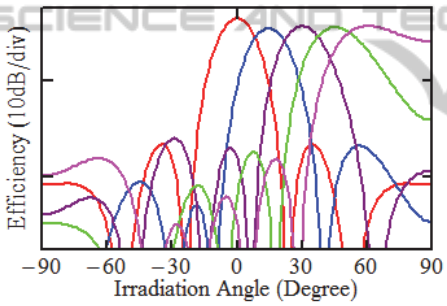

Figure 9: Calculated irradiation angle dependence of the designed QPM EO modulator for several patterns of meandering-gaps.

The meandering-gaps are promising for wireless irradiation angle or beam-forming controls. Several patterns of meandering gaps are designed as shown in Figure 8. The designed meandering gaps are set by considering transit-time effect for receiving several irradiation angles of wireless signals.

The directivity of wireless millimetre-wave signals in the proposed device can be calculated using Equation (3). The calculated directivities in the designed device for several patterns of meandering gaps are shown in Figure 9. Clearly, the meandering gaps can be used for controlling irradiation angle or beam-forming of wireless millimetre-wave signals.

4 EXPERIMENT

4.1 Fabrication Process

The designed device was fabricated. First, a *z*-cut $LiNbO_3$ crystal with a thickness of 250μm was prepared. Then, single-mode orthogonal channel optical waveguides were fabricated on the EO crystal using titanium diffusion method (Hu, 2010). The titanium were diffused with 1100^0C for 10 hours. After that, a 0.2μm-thick SiO_2 buffer layer was deposited on the EO crystal. An array of patch electrodes embedded with orthogonal-gaps was also fabricated on the EO crystal. The patch electrodes were fabricated using a 2μm-thick gold film on the EO crystal through thermal vapor deposition, standard photo-lithography, and a lift-off technique. The optical waveguides were aligned onto one side of the gap edge.

A ground metal was deposited to the bottom surface of a low-*k* dielectric material. Then, the top surface of a low-*k* dielectric material was covered with an optical adhesive for next bonding process.

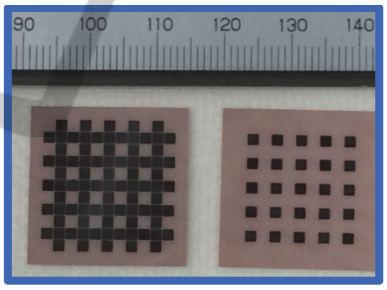

Figure 10: A photograph of the fabricated devices with an array of gap-embedded patch-antennas, (a) with QPM structures and (b) with no QPM structure.

In bonding process, the EO crystal was flipped over with 180 degrees. So as the metal antennas become on the bottom surface of the EO crystal. Then, the flipped EO crystal was bonded to the low-*k* dielectric material by exposing ultraviolet (UV) light to the UV-cured optical adhesive (Uddin, 2006). Finally, the 250μm-thick EO crystal was polished to the designed thickness of 80μm using a polishing machine with diamond slurry. A photograph of the fabricated device is shown in Figure 10.

4.2 Measurement Setup

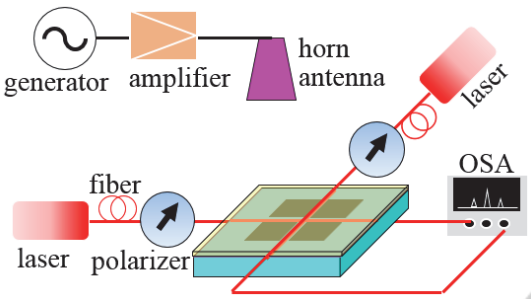

Figure 11: Measurement setup for characterization of the fabricated devices.

Performance of the fabricated device were measured experimentally with a measurement setup as shown in Figure 11. Lights of 1.55μm wavelength from laser were propagated to optical fibres and coupled to the fabricated device. Millimetre-wave signal in 40GHz bands from a signal generator was amplified and irradiated to the fabricated device using a horn antenna with an irradiation power of 20mW. The output lightwave signals were measured using an optical spectrum analyser (OSA).

Typical of the measured output light spectra from two orthogonal waveguides are shown in Figure 12, where a 34GHz wireless millimetre-wave signal was irradiated at the device at a normal irradiation angle and polarization of 45 degree. The optical sidebands were observed clearly. The intensity ratio between the sidebands and optical carrier were about 37dB.

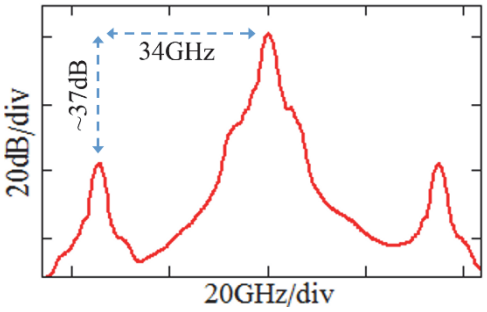

Figure 12: Typical measured output light spectra from the orthogonal waveguides.

The measured modulation efficiency as a function of millimetre-wave frequency is shown by the dots in Figure 13, when the irradiation angle of the wireless millimetre-wave signal was set to be normal to the device. The unit is expressed for power ratio between carrier and sidebands per millimetre-wave irradiation power and distance between the horn antenna and fabricated device. The measured peak frequency was about 34GHz. It is slightly shifted than the designed operational frequency due to fabrication error such as EO crystal thickness, UV-adhesive glue thickness, and other parameters.

The dots in Figure 14 show the measured modulation efficiency as a function of wireless irradiation angle in the *yz*-plane, when the frequency of the wireless millimetre-wave signal was set at 34GHz. The largest modulation efficiency for certain wireless irradiation angle depends on meandering-gap patterns. The measured directivities are in good agreement with the calculation results.

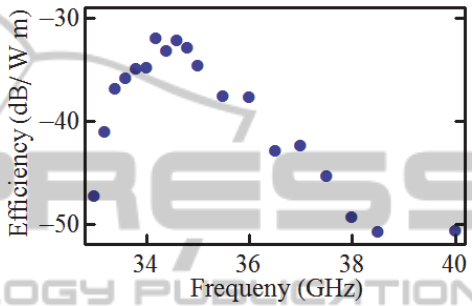

Figure 13: Measured modulation efficiency as a function of the millimetre-wave operational frequency.

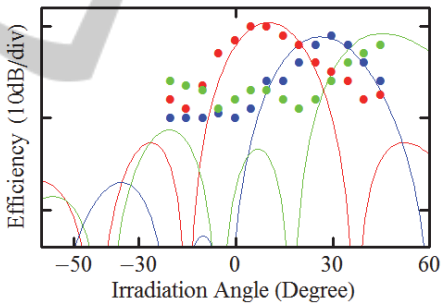

Figure 14: Measured modulation efficiency as a function of wireless millimetre-wave irradiation angles.

5 CONCLUSIONS

Optical modulators with a QPM array of orthogonal-gap-embedded patch-antennas on a low-*k* dielectric material were proposed. A wireless millimetre-wave signal can be received and converted directly to a lightwave signal with the proposed device through EO modulation using the Pockels effect. Performance of the proposed device for operation in the millimetre-wave band was demonstrated experimentally. The proposed device can be operated for dual linear polarization or circular polarization of wireless millimetre-wave signals since orthogonal-gaps are used. Double modulation efficiency can be

obtained also since a QPM array structure is used. The proposed device has a compact structure and can be operated with a low millimetre-wave signal loss and no external electrical power supply.

The proposed device is promising for broadband wireless communication such as for Multi-Input Multi-Output (MIMO) and Space-Division-Multiplexing-Access (SDMA) (Wijayanto, 2013). It can be used also for precise measurement/ sensing applications such as high-frequency Electromagnetic Compatibility (EMC) chamber and Radio Detecting and Ranging (RADAR).

ACKNOWLEDGEMENTS

The authors would like thank to Dr. T. Umezawa from National Institute of Information and Communication Technology (NICT) Japan and Dr. H. Shiomi from Osaka University Japan for their constructive comments and suggestions during discussion. Thanks to Dr. Y. Ogawa from NICT Japan for his helpful supports during device fabrication.

Y. N. Wijayanto, A. Kanno, S. Nakajima, and T. Kawanishi would like thank to the Ministry of Internal Affairs and Communications, Japan, for the financial support partly thru the project entitled "Research and Development of high-precision imaging technology using 90 GHz band linear cells" funded by the "Research and Development to Expand Radio Frequency Resources."

REFERENCES

Abichar, Z., Peng, Y., and Chang, J., "WiMAX: The Emergence of Wireless Broadband," *IEEE Computer Society*, Vols. July-August, pp. 44-48, 2006.

Akyildiz, I. F., Gutierrez-Estevez, D.M., Reyes, E.C., "The evolution to 4G cellular systems: LTE-Advanced," *Physical Communication*, vol. 3, pp. 217-244, 2010.

Bridges, W. B., Sheehy, F.T., and Schaffner, J.H., "Wave-Coupled $LiNbO_3$ Modulator for Microwave and Millimeter-Wave Modulation," *IEEE Photonics Technology Letters*, vol.3, no.2, pp.133-135, February 1991.

Gupta, V. R. and Gupta, N., "Characteristics of a Compact Microstrip Antenna," *Microwave and Optical Technology Letters*, vol.40, no.2, pp.158-160, January 2004.

Hu, H., Ricken, R., Sohler, W., "Low-loss ridge waveguides on lithium niobate fabricated by local diffusion doping with titanium," *Applied Physics B*, vol.98, pp.677–679, 2010.

Iezekiel, S., Microwave photonics: Devices and Applications, John Wiley & Sons Ltd, Chichester, UK, 2009.

Lefort, G., and Razban, T., "Microstrip Antennas Printed on Lithium Niobate Substrate," *Electronics Letters*, vol.33 no.9, pp.726-727, April 1997.

Lu, X., Wang, P., Niyato, D., and Hossain, E., "Dynamic Spectrum Access in Cognitive Radio Networks with RF Energy Harvesting," *IEEE Wireless Communications*, pp. 102-110, Jun. 2014.

Mendeiros, H. P., Maciel, M. C., Sauza, R. D., and Pellenz, M.E., "Lightweight Data Compression in Wireless Sensor Networks Using Human Coding," *International Journal of Distributed Sensor Networks*, vol. 2014, ID 672921, Jan. 2014.

Murata, H., Miyanaka, R., and Okamura, Y., "Wireless Space-Division-Multiplexed Signal Discrimination Device Using Electro-Optic Modulator with Antenna-Coupled Electrodes and Polarization-Reversed Sructures," *International Journal of Microwave and Wireless Technologies*, vol.4, pp.399-405, April 2012.

Pi, Z. and Khan, F., "An introduction to millieter-wave mobile broadband systems," *IEEE Communications Magazine*, vol. June 2011, pp. 101-107, 2011.

Recsi. ITU-R P.676-5, "Attenuation of atmospheric gases," 2001.

Rodriguez-Berral, R., Mesa, F., and Jackson, D. R., "Gap Discontinuity in Microstrip Lines: An Accurate Semi analytical Formulation," *IEEE Transactions on Microwave Theory and Techniques*, vol.59, no.6, pp, 1441-1453, June 2011.

Shi, J., Huang, C., and Pan, C., "Millimeter-wave photonic wireless links for very high data rate communication," *NPG Asia Materials*, vol.3, pp.41, April 2011.

Seeds, A. J., "Microwave Photonics," *IEEE Transactions on Microwave Theory and Techniques*, vol.50, no.3, pp.877-887, March 2002.

Shinada, S., Kawanishi, T., and Izutsu, M., "A Resonant Type $LiNbO_3$ Optical Modulator Array with Micro-Strip Antennas," *IEICE Transactions on Electronics*, vol.E90-C, no.5, pp.1090-1095, May 2007.

Sheehy, F. T., Bridges, W. B., and Schaffner, J. H., "60 GHz and 94 GHz Antenna-Coupled $LiNbO_3$ Electrooptic Modulators," *IEEE Photonics Technology Letters*, vol.5, no.3, pp.307-310, March 1993.

Uddin, M. A., Chan, H. P., Tsun, T. O., and Chan, Y. C., "Uneven Curing Induced Interfacial Delamination of UV Adhesive-Bonded Fiber Array in V-Groove for Photonic Packaging," *Journal of Lightwave Technology*, vol.24, no.3, pp.1342-1349, March 2006.

Watanabe, I., Nakata, T., Tsuji, M., Makita, K, Torikai, T., and Taguchi, K., "High-Speed, High-Reliability Planar-Structure Superlattice Avalanche Photodiodes for 10-Gb/s Optical Receivers," *Journal of Lightwave Technology*, vol.18, no.12, pp. 2200- 2207, December 2000.

Wijayanto, Y. N., Murata, H., and Okamura, Y., "Novel Electro-Optic Microwave-Lightwave Converters Utilizing a Patch-antenna Embedded with a Narrow

Gap," *IEICE Electronics Express*, vol.8, no.7, pp.491-497, April 2011.

Wijayanto, Y. N., Murata, H., Kawanishi, T., and Okamura, Y., "*X*-Cut $LiNbO_3$ Optical Modulators Using Gap-Embedded Patch-Antennas for Wireless-Over-Fiber Systems," *Advances in Optical Technologies*, vol. 2012, Article ID 383212, 8 pages, 2012.

Wijayanto, Y. N., Murata, H., and Okamura, Y., "Electro-Optic Beam Forming Device Using a Two-Dimensional Array of Patch-Antennas Embedded with Orthogonal-Gaps for Millimeter-Wave Signals," IEEE Photonic Conference 2013, Seattle, 2013.

Yariv, A., Quantum Electronics, 3rd ed., Wiley, New York, 1989.